

Month 2018 Protic Ionic Liquid Promoted One Pot Synthesis of 2-amino-4-(phenyl)-7-methyl-5-oxo-4*H*,5*H*-pyrano[4,3-*b*]pyran-3-carbonitrile Derivatives in Water and Their Antimycobacterial Activity

Priyanka P. Mohire,<sup>a</sup> Dattatray R. Chandam,<sup>b</sup> Reshma B. Patil,<sup>a</sup> Digambar R. Kumbhar,<sup>a</sup> Sunetra J. Jadhav,<sup>a</sup> Ajinkya A. Patravale,<sup>c</sup> Vijaya P. Godase,<sup>d</sup> Jai S. Ghosh,<sup>a</sup> and Madhukar B. Deshmukh<sup>a,c,\*</sup> 

<sup>a</sup>Chemistry Research Laboratory, Department of Agrochemicals & Pest Management, Shivaji University, Kolhapur, Maharashtra 416004, India

<sup>b</sup>Department of Chemistry, Bhogawati Mahavidyalaya, Kurukali, Kolhapur, Maharashtra 416001, India

<sup>c</sup>Department of Chemistry, Vivekananda College Kolhapur, Kolhapur, Maharashtra 416004, India

<sup>d</sup>Biochemistry Research Laboratory, Institute of Bioinformatics and Biotechnology, Savitribai Phule University, Pune, Maharashtra 411007, India

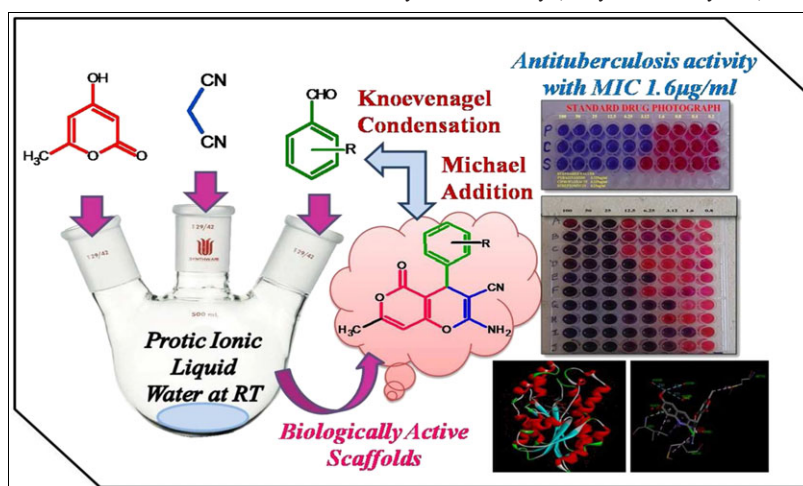
\*Heterocyclic Chemistry Laboratory, Department of Chemistry, Shivaji University, Kolhapur, Maharashtra 416004, India

\*E-mail: shubhlaxmi111@gmail.com

Received November 11, 2017

DOI 10.1002/jhet.3133

Published online 00 Month 2018 in Wiley Online Library (wileyonlinelibrary.com).



One pot three component reaction of 4-hydroxy-6-methylpyran-2-one, 3-methoxy benzaldehyde, and malononitrile in water using protic ionic liquid as a catalyst at room temperature afforded pyrano[4,3-*b*]pyran derivatives. Protic ionic liquid has been proved to be an efficient and mild catalyst for the synthesis of pyrano[4,3-*b*]pyran scaffolds due to their highly polar nature. The notable aspects of protic ionic liquid are easy availability, improved reaction rates, high product yields, simple workup procedure, recyclability, and reusability. Molecules docking studies have been performed on enzyme enoyl-ACP-reductase from *Mycobacterium tuberculosis*. The molecular docking simulation indicated plausible  $\pi$ -alkyl and alkyl-alkyl interactions between the amino acids and scaffolds. The synthesized derivatives have been evaluated for their *in vitro* antitubercular activity against *M. tuberculosis* H<sub>37</sub>RV strain using Microplate Alamar Blue Assay method. Together, biological activity data and docking data showed that the tested scaffolds exhibited excellent antitubercular activity.

*J. Heterocyclic Chem.*, 00, 00 (2018).

## INTRODUCTION

Tuberculosis is caused by pathogenic bacteria *Mycobacterium tuberculosis*. It is a chronic infectious disease that infects with one-third of the world's population. Currently, TB is treated with a first-line-drug regimen including mainly isoniazid, rifampicin, pyrazinamide, and ethambutol for 6 month dosage [1–3]. According to the report of World Health Organization in 2015, worldwide 10.4 million TB cases were found [4]. In all, tuberculosis has been a global health problem for developing countries including India. Today, this epidemic

disease remains main problems of medicinal and social point of vision because of emergence of multidrug-resistant strains of *M. tuberculosis* and extensively drug-resistant TB [5–7]. Therefore, to fight this problem, our interest is to discover a new protocol for the synthesis of new antimycobacterial agents. Virtual analysis of the molecules is the computational methodology in which the macro and micro molecular interactions were tested. The enoyl-ACP-reductase plays an important role in the synthesis of fatty acid by utilizing reduced nicotinamide adenine dinucleotide (NADH) to reduce double bond of trans-2 enoyl-ACP [8]. The InhA is enoyl-ACP-reductase from

*M. tuberculosis* acts as key enzyme in the biosynthesis of mycolic acid and in the formation of mycobacterial cell wall. The primary antitubercular drug Isoniazid, targeted on the NADH dependant enoyl-ACP-reductase [9,10]. Considering the vital applications of heterocycles like coumarins, pyrans, pyrimidines, quinoline substituent, and natural products against *M. tuberculosis* has significant importance due to their biocompatibility as well as lower toxicity [11–13]. In this work, we performed the molecular docking analysis of the synthesized scaffolds.

Last decade, green chemistry has been proved be an efficient pathway for the synthesis of heterocyclic compounds and also beneficial to other related fields. By multi-component reactions, the desired products can be achieved in one step using eco-friendly techniques and no revelation to environment [14]. In modern era, multicomponent reactions offer an easy route to develop combinatorial chemistry procedures and to synthesize biological scaffolds possessing diversity and complexity in agricultural and pharmaceutical areas with advantages such as environmentally beneficial, operational simplicity, high yield of the products with no chromatographic purification, high atom economy, and facile execution [15–20].

Protic ionic liquid (PIL) is a subclass of ILs that is prepared by the stoichiometric neutralization reaction of certain Bronsted acids and bases [21–23]. PILs have been reported as the recyclable solvents for the acid catalyzed synthesis of diphenylmethyl thioethers [24], also reported that the reusability and highly catalytic efficiency for the formylation of amines [25]. DABCO: AcOH: H<sub>2</sub>O solvent-catalyst system also evaluated for the Baylis-Hillman reaction [26]. Recently, different PILs reported as a recyclable solvent as well as catalyst for the organic syntheses and condensation reactions [27–29]. Various organic and multicomponent reactions are reported in PILs [30–34]. The main features of the PILs such as, negligible vapor pressure and thermal stability. The reusability is a key characteristic of PIL and can be used as a green alternative solvent [35,36].

In recent time, pyrano-pyran and pyrano-chromene derivatives have attracted attention due to their pharmacological as well as biological activities such as

fungicidal, insecticidal [37,38], antiviral and antileishmanial [39], anticonvulsant [40], antibacterial [41], and antituberculosis activity (Fig. 1) [42–45].

Thus, there has been a rising significance of developing a general and diverse method for the synthesis of pyrano[4,3-*b*]pyran derivatives. A number of synthetic approaches have been introduced in recent years [46]. As per the literature survey, few methods were reported for the synthesis of pyrano[4,3-*b*]pyran derivatives using a variety of reagents [47–54] have been employed to accomplish this transformation. But several methods have some limitations such as time consuming reaction path, lower yields, use of organic solvents, complex workup procedure, and non-recyclability of the catalyst.

Considering, all points that mentioned above, our interest to develop a new protocol for the synthesis of pyrano[4,3-*b*]pyran derivatives using green chemistry principles and screening them against antituberculous activity. We utilized recyclable PILs DABCO: AcOH: H<sub>2</sub>O (1:1:3) for the synthesis of prominent molecules like pyranopyrans.

## RESULT AND DISCUSSION

**Chemistry.** Protic ionic liquid is easily prepared by Bronsted acid (Acetic acid) and base (DABCO) that proved to be efficient catalyst for the synthesis of various diverse heterocyclic derivatives in shorter reaction time [33].

In initial study, we have used 4-hydroxy-6-methyl pyran-2-one, 3-methoxy benzaldehyde, and malononitrile, the model reaction using PIL (20 mol%) as a catalyst at a room temperature (Scheme 1). After the completion of reaction as monitored by thin layer chromatography

**Scheme 1.** Synthesis of 2-amino-4-(aryl)-7-methyl-5-oxo-4*H*,5*H*-pyrano[4,3-*b*]pyran-3-carbonitrile. [Color figure can be viewed at [wileyonlinelibrary.com](http://wileyonlinelibrary.com)]

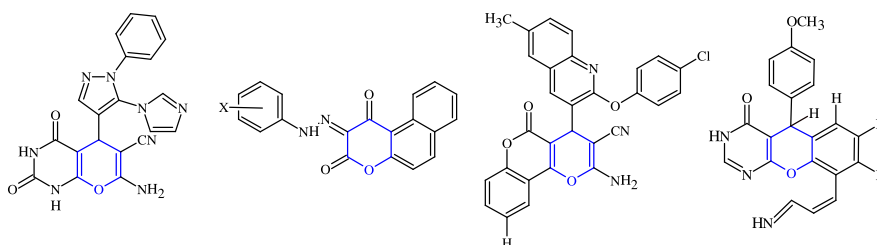
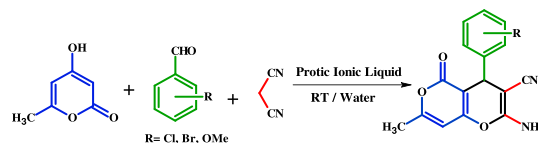


**Figure 1.** Various pyran scaffolds exhibiting antituberculous activity. [Color figure can be viewed at [wileyonlinelibrary.com](http://wileyonlinelibrary.com)]

(TLC), crude product formed 2-amino-4-(3-methoxyphenyl)-7-methyl-5-oxo-4*H*,5*H*-pyrano[4,3-*b*]pyran-3-carbonitrile was filtered and washed with hot water and recrystallized in ethanol and further characterized by spectral analysis.

Inspired by these results, the reaction was carried out in the presence of a variety of catalysts and solvents under different conditions. We observed that in the presence of various acid catalyst and base catalyst, desired results were not obtained means reaction proceeds up to Knoevenagel condensation. On the other side, DABCO, acetic acid with water combination as a catalyst endowed better yield in less time. We also endeavor various proportions of DABCO, acetic acid, and water (Table 1, entries 9–11) and found that 1:1:3 were the most efficient proportion might be due to its viscous nature. In addition to this, we also tried the salts of DABCO with different weak acids such as cinnamic acid, benzoic acid (Table 1

entries 7–8), however, the results were unsatisfactory. The results obtained are summarized in (Table 1).

To study the solvent efficiency, the reaction was carried out in a variety of polar and nonpolar solvents (Table 2). But the representative reaction failed to proceed beyond the Knoevenagel condensation product. The formation of the product was also demonstrated under refluxing conditions. The reaction was incomplete even after 5 h (Table 2, entry 5).

Thus, at room temperature, all the components in presence of [DABCO: AcOH: H<sub>2</sub>O] (1:1:3) in water are proved to be the optimum conditions for this reaction. Using these optimized reaction conditions, series of pyrano[4,3-*b*]pyran derivatives (Table 3) were prepared in an excellent yields from different aryl aldehydes having electron donating as well as electron-withdrawing groups.

**Table 1**  
Influence of catalyst on the synthesis of (Entry 5)<sup>a</sup>.

Sr. no.	Catalyst	Catalyst (mol %)	Reaction time (min.)	Yield (%) <sup>b</sup>
1	PTSA	20	120	Knoevenagel product
2	CuO	20	55	Knoevenagel product
3	P <sub>2</sub> O <sub>5</sub>	20	90	40
4	AcOH	—	60	44
5	Sulfamic acid	20	3 h	52
6	DABCO	20	60	42
7	DABCO-PhCOOH-H <sub>2</sub> O (1:1:3)	—	240	Knoevenagel product
8	DABCO-Cinnamic acid-H <sub>2</sub> O (1:1:3)	—	180	38
<b>9</b>	<b>DABCO-AcOH-H<sub>2</sub>O (1:1:3)</b>	<b>20</b>	<b>20</b>	<b>94</b>
10	DABCO-AcOH-H <sub>2</sub> O (1:1:5)	—	60	78
11	DABCO-AcOH-H <sub>2</sub> O (1:1:7)	—	120	65

Highest yield in shortest reaction time shown in bold.

<sup>a</sup>Reaction condition: 4-hydroxy-6-methylpyran-2-one (1 mmol), malononitrile (1 mmol), and 3-methoxy benzaldehyde (1 mmol) at room temperature in respective catalyst.

<sup>b</sup>Yields refer to pure isolated products.

**Table 2**  
Influence of solvent on the synthesis of (Entry 5)<sup>a</sup>.

Sr. no.	Solvent	Temp. condition	Reaction time (min.)	Yield (%) <sup>b</sup>
1	Ethanol	R.T	120	Knoevenagel product
<b>2</b>	<b>Water</b>	<b>R.T</b>	<b>20</b>	<b>94</b>
3	Acetonitrile	R.T	120	32
4	Water: Ethanol (8:2)	R.T	180	45
5	Water: Ethanol(1:1)	R.T	240	Knoevenagel product
6	Ethanol	Reflux (80°C)	80	Knoevenagel product
7	Water	Reflux (80°C)	120	60
8	Acetonitrile	Reflux (80°C)	120	56
9	Water: Ethanol (8:2)	Reflux (80°C)	80	64

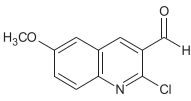
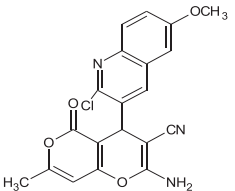
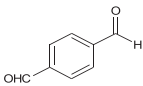
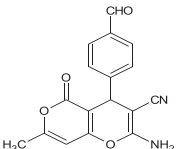
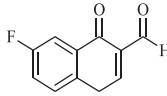
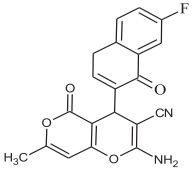
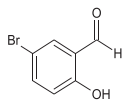
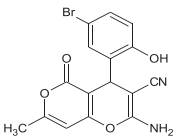
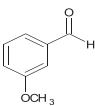
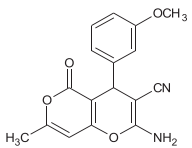
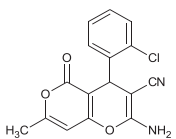
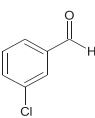
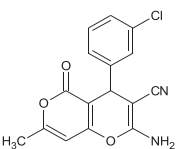
Highest yield in shortest reaction time shown in bold.

<sup>a</sup>Reaction condition: 4-hydroxy-6-methylpyran-2-one (1 mmol), malononitrile (1 mmol), and 3-methoxy benzaldehyde (1 mmol) at room temperature in 5 mL respective solvent.

<sup>b</sup>Yields refer to pure isolated products.

**Table 3**

Synthesis of 2-amino-4-(phenyl)-7-methyl-5-oxo-4*H*,5*H*-pyrano[4,3-*b*]pyran-3 carbonitrile derivatives using protic ionic liquid as a catalyst. (Entry 1–13)<sup>a</sup>.

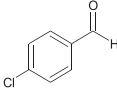
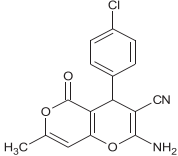
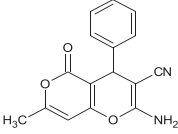
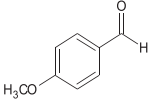
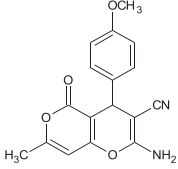
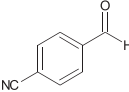
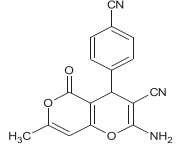
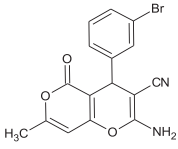
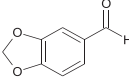
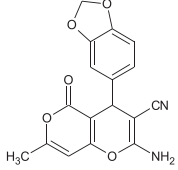
Sr. no.	Aldehydes	Product	Time (mins)	Yield (%)	M.P.		Ref.
					Found	Reported	
1			35	88	>300	—	
2			35	84	270	—	
3			40	90	>300	—	
4			30	87	282	—	
5			20	94	238	233–235	[32-b]
6			25	90	268	266–268	[29]
7			25	93	256	254–256	[31]

(Continues)

The noteworthy feature of this methodology is that it works well for hetero-aromatic aldehydes (Table 3). The hydrogen bonding nature of PIL initiates the electrophilic

activation of carbonyl group of aromatic aldehyde. Further Knoevenagel condensation of substituted aldehyde and malononitrile takes place. Further, the aza-

**Table 3**  
(Continued)

Sr. no.	Aldehydes	Product	Time (mins)	Yield (%)	M.P.		Ref.
					Found	Reported	
8			20	92	232	228–230	[32]
9			20	88	236	236	[32]
10			30	80	214	210–212	[32-a]
11			35	86	228	230–232	[32-b]
12			30	83	216	217–219	[32-a]
13			25	92	264	—	

<sup>a</sup>Reaction condition: 4-hydroxy-6-methylpyran-2-one (1 mmol), malononitrile (1 mmol), and 3-methoxy benzaldehyde (1 mmol) at room temperature in 5 mL water with PIL as a catalyst.

<sup>b</sup>Yields refer to pure isolated products.

Michael addition forms the ring oxygen of the 4-hydroxy 6-methyl 2-pyrone leads to the formation of intermediary aza-Michael adduct followed by intramolecular cyclization to yield the final product (Scheme 2).

The present methodology compared with previously reported procedures for the synthesis of pyrano[4,3-*b*]pyran is shown in (Table 4). It can be seen that the reaction catalyzed by PILs at room temperature gave a promising yields in water, with less amount of catalyst

and time than the other protocols, with reusability of the catalyst.

**Reusability of catalyst.** Recyclability and recovery of a catalyst is a noteworthy aspect from commercial point of view and demonstrate green aspects of the protocol. Recovery of the catalyst in reaction medium was investigated by using the model reaction. Thus, we studied the recyclability of the catalyst [DABCO: AcOH: H<sub>2</sub>O] in the reaction. After the reaction was completed,

**Scheme 2.** Mechanistic pathway of the 2-amino-4-aryl-7-methyl-5-oxo-4,5-dihydropyrano[4,3-*b*]pyran-3-carbonitriles in presence of PIL as a catalyst.

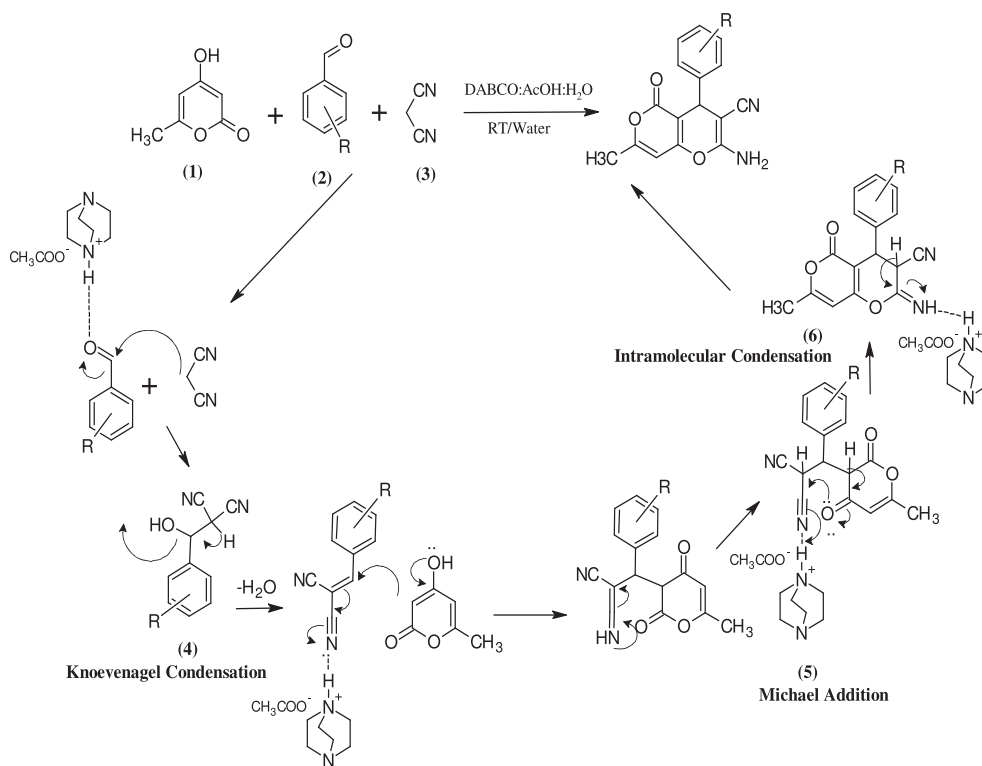


**Table 4**

Optimization of catalyst with reported catalysts.

Entry	Catalyst	Conditions	Time (min.)	Yield (%)	Ref.
1	Piperidine (1–2 drops)	MeOH, reflux	60	79	[41]
2	TMGT (1 mol %)	100°C	60	77	[42]
3	KF-Al <sub>2</sub> O <sub>3</sub>	EtOH, R.T	480	76	[43]
4	MgO (0.25 g)	H <sub>2</sub> O/EtOH, reflux	30	89	[44]
5	H <sub>6</sub> P <sub>2</sub> W <sub>18</sub> O <sub>62</sub> ·18H <sub>2</sub> O (1 mol %)	H <sub>2</sub> O, reflux	60	94	[45]
6	[BBMIm](HSO <sub>4</sub> ) <sub>2</sub> (500 mg)	Neat, 60°C	35	94	[46]
7	Thiourea dioxide (TUD)	H <sub>2</sub> O, 80°C	40	92	[47]
8	SBSA (4.2 mol %)	Neat, 60°C	60	88	[48]
<b>9</b>	<b>DABCO: AcOH: H<sub>2</sub>O (1:1:3)</b>	<b>Water, R.T</b>	<b>20</b>	<b>94</b>	<b>This work</b>

Highest yield in shortest reaction time shown in bold.

the product was collected simply by filtration and recrystallized. The removal of extra water from filtrate under reduced pressure recovered the catalyst system (90%), washed with toluene, and reused for three times as in Figure 2.

**Green metric calculations.** In accordance with green chemistry principles, green metrics such as mass intensity (MI), reaction mass efficiency (RME), carbon efficiency (CE), and atom economy (AE) and E Factor have been considered as a measure of environmental sustainability in diminishing the amount of theoretical waste [55,56]. In ideal condition MI  $\approx$  1%, RME  $\approx$  100%, %CE  $\approx$  100 and %AE  $\approx$  100, and E-factor  $\approx$  0 is expected [57–59]. To

reveal the greenness of the present protocol, we have shown green metrics calculations for synthesized derivatives in (Table 5) MI values of all derivatives obtained are quite excellent. The high yield of the products demonstrates that the significant RME values and moderate yield generate moderate RME values. In addition to this, all carbon atoms in the reactants are present in the product that shows excellent values of % CE. MI values and E factor of the reaction are very close to the ideal values. The percent AE of each scaffold is a sign of maximum conversion of starting materials into product and minimum waste exclusion. Mass of catalyst is excluded as it is recyclable. Table 5 itself points

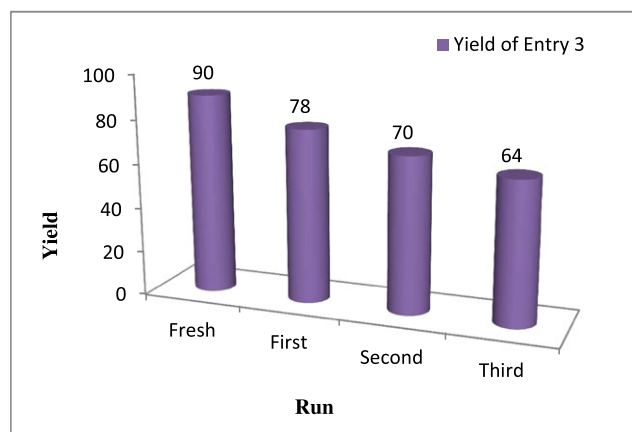


Figure 2. Recyclability of catalyst. [Color figure can be viewed at wileyonlinelibrary.com]

Table 5  
Green Metrics Calculations for (Entry 1–13).

Entry no.	Compound Code	% Yield	FW Product	Yield (g)	MI	% RME	% CE	% AE	E-factor
1	PA	88	395.79	0.348	1.18	84.26	88	84.16	0.18
2	PB	84	308.28	0.258	1.24	80.62	84	80.84	0.23
3	PC	90	364.32	0.342	1.11	85.60	90	85.75	0.16
4	PD	87	375.17	0.326	1.20	82.95	87	83.00	0.20
5	PE	94	310.30	0.291	1.12	88.71	94	88.83	0.13
6	PF	90	314.72	0.282	1.17	84.93	90	85.12	0.17
7	PG	93	314.72	0.292	1.13	87.95	93	87.95	0.13
8	PH	92	314.72	0.288	1.15	86.74	92	87.01	0.14
9	PI	88	280.27	0.246	1.21	82.55	88	82.68	0.20
10	PJ	80	310.30	0.248	1.32	75.60	80	75.60	0.32
11	PK	86	305.28	0.262	1.25	79.87	86	81.27	0.25
12	PL	83	359.17	0.297	1.26	78.77	83	78.36	0.26
13	PM	92	324.28	0.298	1.14	87.13	92	79.09	0.14

towards the present protocol of the reaction having noteworthy green metrics correlation.

**Virtual screening. Docking simulation.** In silico screening of pyrano[4,3-*b*]pyran, scaffolds were docked on with NADH-dependent enoyl-ACP-reductase was carried out with the docking parameters. Initial blind docking of individual compound generated 90 poses each. Of these, blind poses possessing minimal energy docked near the active pocket. The subsequent refined docking of the compounds generated the best poses with minimal energy of interaction shown in Table 6. The molecular docking simulation indicated plausible  $\pi$ -alkyl and alkyl-alkyl interactions between the amino acids and scaffolds. These interactions of pyrano[4,5-*b*]pyran active lead molecules with enoyl-ACP-reductase are depicted in the following (Figs. 3 and 4).

Compound code **PA** showed one aromatic interaction with PHE149 and hydrogen bond interactions with SER20, GLY14, GLY96, and MET98. **PA** also exhibited hydrophobic as well as Van der Waals interaction with

ILE21, MET147, ALA191, PRO193, MET199, MET103, MET161, LYS165, and THR196. **PB** (Fig. 4), **PC** (Fig. 5), and **PD** (Fig. 6) have been exhibited common aromatic interaction with PHE41. **PB** and **PC** showed hydrogen bond interaction with amino acid GLY96. The compound codes **PB**, **PC**, **PD**, and **PE** have also reveal the hydrophobic and Van der Waals interaction with MET147. On the basis of molecular docking, **PA** molecule shows all type of interactions in the virtual screening. (Remaining docking figures are included in the Supporting Information).

The interactions of **PA** structure with an enzyme enoyl-ACP-reductase include alkyl interaction between ILE16, ILE95, MET147, MET103, and ALA198 with bond lengths of 5.45, 3.96, 4.56, 4.45, 4.00Å, respectively. The compound also exhibits pi-alkyl interaction between ILE21, PHE97 with bond length of 4.30, 5.16Å correspondingly. Conventional hydrogen bonding with a bond length of 2.05 and 1.29Å was observed between HOH352.

**Table 6**  
Interactions of pyrano[4,5-*b*]pyran lead molecules with enoyl-ACP-reductase.

Compound code	Interactions with amino acids			Affinity (kcal/mol)	Binding mode out of 100 modes	
	Hydrogen bond interaction	Aromatic interaction	Hydrophobic and van der Waals interaction			
<b>PA</b>	SER20, GLY14, GLY96, MET98, HOH	PHE149	ILE21, ALA191, MET199, MET161, THR196	MET147, PRO193, MET103, LYS165,	-9.0	1
<b>PB</b>	GLY96, GLY192, ALA22, SER94, HOH	PHE41	GLY14, ILE122, ILE16, SER20, MET147, ASP148, ILE21, THR196,	VAL65, ILE95, ILE47, MET199, ASP64, GLN66, THR39,	-9.8	2
<b>PC</b>	GLY192, GLY96, HOH,	PHE41, PHE97, TYR158	THR 196, GLY14, ILE21, MET199, ILE95, GLY14	SER94, ASP148, MET147, ILE202, ILE16,	-9.5	2
<b>PD</b>	LYS165, SER94, GLY96	PHE41	SER94, ILE21, MET161, ALA191,	ILE95, GLY96, MET147, ASP148	-7.7	1
<b>PE</b>	LYS165, ILE194, GLY196	TYR158, PHE149, PHE97	SER94, MET147, GLY192 ASP148,	GKY96, ILE21, ALA191, MET161	-9.3	10
<b>PF</b>	SER94	PHE97, PHE41, PHE149	ILE122, ILE21, GLY14, LYS118, LYS165, SER20	ILE15, ILE95, GLY96, MET147, MET161,	-8.1	1
<b>PG</b>	GLU196	PHE97, PHE41	ILE122, ASP148, MET161, ILE16, THR39,	ILE21, SER20, MET198, GLY14,	-9.6	1
<b>PH</b>	PHE41, GLY96, ILE15, THR196	TYR158, PHE149,	IL122, GLY40, ILE95, MET161, THR39,	ILE16, GLY14, SER94, MET98, VAL65	-10.0	1
<b>PI</b>	GLY96,	PHE41, PHE149,	ILE16, ILE122, THR39, LYS165, ILE194,	GLY14, ILE95, ILE47, MET147, THE196	-9.6	6
<b>PJ</b>	GLY96, ILE21,	PHE49, PHE41, TYR158, PHE149	VAL65, ILE122, ILE16, ILE47, MET161, SER20,	ASP64, ILE95, GLY14, THR39, THR196, ASP148	-9.4	1
<b>PK</b>	GLY96, THR196	PHE149, TYR158	ILE95, ASP64, ILE15, ILE47,	ILE122, VAL65, GLY14, SER94,	-10.3	1

(Continues)

**Table 6**  
(Continued)

Compound code	Interactions with amino acids			Affinity (kcal/mol)	Binding mode out of 100 modes	
	Hydrogen bond interaction	Aromatic interaction	Hydrophobic and van der Waals interaction			
<b>PL</b>	GLY96, THR196, ASP148	PHE97, PHE41, PHE149, TYR158	MET 161, ILE122, SER94, ILE21, ILE202,	MET199, ILE95, MET147, MET161, GLY14,	-9.3	6
<b>PM</b>	SER94, ILE21	TYR158, PHE149,	GLY14, ALA191, MET161, GLY96	MET147, THR196, ASP148,	-8.8	1

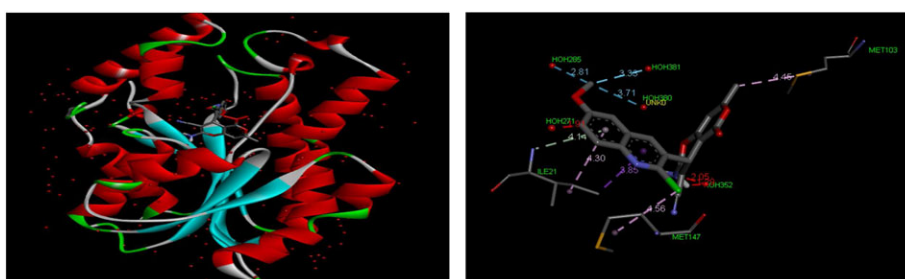


**Figure 3.** Significant interaction of molecule **PA** with NADH-dependent enoyl-ACP-reductase. NADH, reduced nicotinamide adenine dinucleotide. [Color figure can be viewed at wileyonlinelibrary.com]

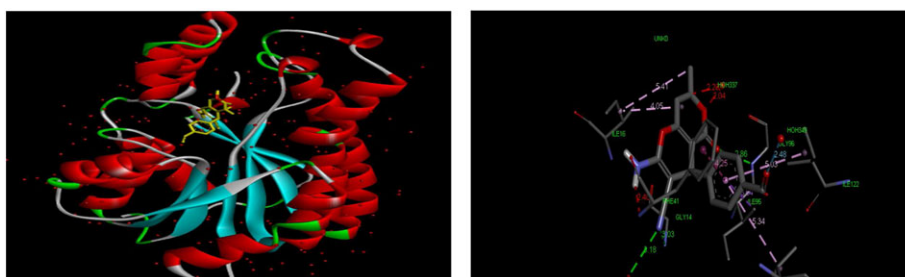


**Figure 4.** Significant interaction of molecule **PB** with NADH-dependent enoyl-ACP-reductase. NADH, reduced nicotinamide adenine dinucleotide. [Color figure can be viewed at wileyonlinelibrary.com]

Another compound **PB** shows the pi-alkyl interaction between ILE122 with bond length 5.03, 5.34Å° with same enzyme. The structure also includes alkyl interaction between ILE16, ILE202 with a bond distance 4.05 and 5.41, 5.19Å°, respectively. Also, conventional hydrogen bonding with a bond length of 2.48 and 3.36Å° was observed between HOH349, HOH352.

**Antituberculosis activity.** A new series of 2-amino-4-aryl-7-methyl-5-oxo-4*H*,5*H*-pyrano[4,3-*b*]pyran-3-carbonitrile were synthesized in good to excellent yield (Scheme 1). All the newly synthesized scaffolds were screened for their antimycobacterial activity against *M. tuberculosis* using Microplate Alamar Blue Assay. The experimental procedure used for antituberculous activity as per reported method in the literature [60]. This

methodology is nontoxic, involves the use of thermally stable reagent, and shows good correlation with proportional and BACTEC radiometric method. The BACTEC (Becton, Dickinson and Company, Franklin Lakes, NJ) is a totally automatic radiometric instrument that utilizes the fluorescence of an oxygen sensor to indicate the growth of *Mycobacteria* in the culture [61].

The Pyrazinamide, Streptomycin and Ciprofloxacin (Table 7, Sr. No.11–13) were used as the standard besides newly synthesized derivatives. The compounds (Table 7, Sr. No.1–10) were tested for antituberculosis activity from 100 to 0.8 µg/mL concentration against *M. tuberculosis* H<sub>37</sub>RV strain (ATCC-27294). All the selected molecules showed profound biological activity against *M. tuberculosis* (H<sub>37</sub>RV strain) using Microplate

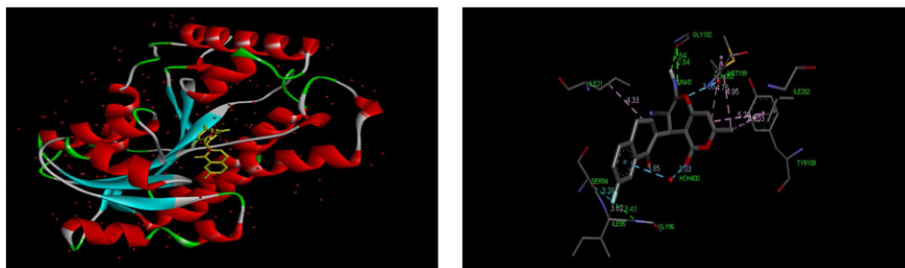


**Figure 5.** Significant interaction of molecule **PC** with NADH-dependent enoyl-ACP-reductase. NADH, reduced nicotinamide adenine dinucleotide. [Color figure can be viewed at wileyonlinelibrary.com]

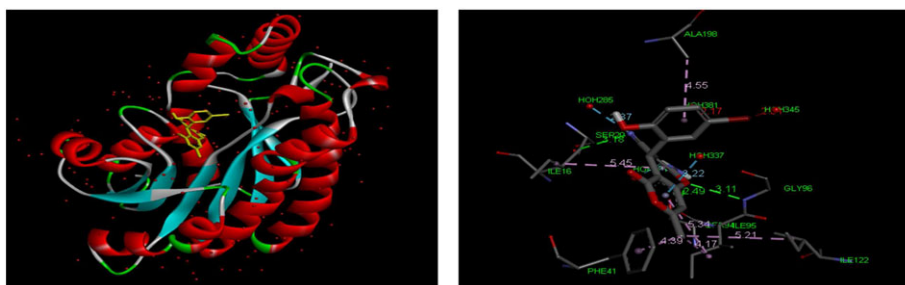


**Figure 6.** Significant interaction of molecule **PD** with NADH-dependent enoyl-ACP-reductase. NADH, reduced nicotinamide adenine dinucleotide. [Color figure can be viewed at wileyonlinelibrary.com]

**Table 7**  
Antituberculosis activity.

Sr. no.	Entry from table no. 3	100 µg/mL	50 µg/mL	25 µg/mL	12.5 µg/mL	6.25 µg/mL	3.125 µg/mL	1.6 µg/mL	0.8 µg/mL
1	<b>PK</b>	S	S	S	R	R	R	R	R
2	<b>PH</b>	S	S	S	R	R	R	R	R
3	<b>PI</b>	S	S	S	R	R	R	R	R
4	<b>PJ</b>	S	S	S	S	R	R	R	R
5	<b>PE</b>	S	S	S	S	S	R	R	R
6	<b>PM</b>	S	S	S	S	R	R	R	R
7	<b>PC</b>	S	S	S	S	S	S	R	R
8	<b>PD</b>	S	S	S	S	S	R	R	R
9	<b>PA</b>	S	S	S	S	S	S	S	R
10	<b>PB</b>	S	S	S	S	S	S	R	R
11	Pyrazinamide	MIC at 12.5 µg/mL							
12	Ciprofloxacin	MIC at 12.5 µg/mL							
13	Streptomycin	MIC at 25 µg/mL							

S, sensitive; R, resistance; MIC, minimum inhibitory concentration.

Alamar Blue Assay. In detail, the entry **PA** that reveals the excellent activity initially from 1.6 µg/mL. Moreover, compounds **PB** and **PC** were superior active against anti-TB with sensitivity up to 3.25 µg/mL whereas the entry **PE** showed moderate activity up to 6.25 µg/mL.

## CONCLUSION

In summary, we have demonstrated an elegant protocol for the synthesis of a variety of pharmaceutical and

agrochemical interesting functionalized pyrano[4,3-*b*]pyran in good to an excellent yields using PIL as an efficient catalyst at room temperature. The procedure is very straightforward that involves the simple filtration product without chromatographic purification. The use of green, nontoxic, economical, and reusable catalyst makes this protocol an attractive choice for the synthesis of such scaffolds. The results obtained from virtual screening and the antituberculous activity of lead molecule obtained against *M. tuberculosis* (H<sub>37</sub>RV strain) using Alamar Blue Assay. Pyrano[4,3-*b*]pyran derivatives

showed an excellent activity. Alamar Blue Assay is a good biological method to check the antituberculosis activity of compounds. The recent study will motivate medicinal chemists to find new better drug like chemical entities among the structures for the treatment of multi-drug resistant tuberculosis.

## EXPERIMENTAL SECTION

**Molecular docking.** Molecular docking analysis was carried out to identify the mode of action of synthesized derivatives using crystal structure of NADH-dependent enoyl-ACP-reductase from *M. tuberculosis* in complex with NADH. (PDBID: 2AQ8). Prior docking analysis, all molecules were drawn in 2D and converted to 3D using Online SMILES Translator and Structure File Generator (<https://cactus.nci.nih.gov/translate/>). Crystal structure of NADH-dependent enoyl-ACP-reductase was downloaded from [www.rcsb.org](http://www.rcsb.org).

Docking simulations of synthesized compounds with NADH-dependent enoyl-ACP-reductase (PDBID: 2AQ8) were performed using AutoDockVina [62]. Blind docking and refine docking was done with the grid box spacing of 0.375 Å. A grid box parameters of 100 × 98 × 104 points, encompassing the NADH-dependent enoyl-ACP-reductase molecule was used for blind docking for all the compounds, whereas refine docking simulation were done with grid parameters that scored high in blind docking. Grid box parameters 30 × 36 × 42 points used for all synthesized derivatives. The interactions of ligands-NADH-dependent enoyl-ACP-reductase were analyzed and visualized in Discovery Studio 4.0 client [63].

**General.** All the chemicals were purchased from Alfa Aesar and Spectrochem (PVT. Ltd, Mumbai, India) and used without purification. The reaction was monitored by TLC. The desired structures of all of the compounds were confirmed by their relevant spectral data. The melting points were determined in open glass capillary tubes were found to be uncorrected. The compounds were confirmed by IR, <sup>1</sup>H NMR, and <sup>13</sup>C NMR. The IR spectra were recorded on a JASCO FT-IR 4600 spectrum spectrophotometer and the values are expressed as  $\nu$  max  $\text{cm}^{-1}$ . The <sup>1</sup>H NMR and <sup>13</sup>C NMR spectra were recorded on Bruker Spectrospin Avance II-300 and 75 MHz spectrophotometer relative to tetramethylsilane as an internal standard using DMSO-*d*<sub>6</sub> as a solvent.

**General synthetic procedure.** A mixture of malononitrile (1 mmol) and aromatic aldehyde (1 mmol) were mixed together in 50 mL round bottomed flask at a room temperature to get the Knoevenagel product monitored by TLC and then 4-hydroxy-6-methylpyran-2-one (1 mmol) and PIL [DABCO: AcOH: H<sub>2</sub>O] (1:1:3)

were added and the reaction mixture stirred at room temperature by using water as a solvent (5 mL) for 15 min. The progress of the reaction was monitored by TLC using solvent system petroleum ether: ethyl acetate (8:2 *v/v*). After the completion, the product was precipitated in round bottomed flask was collected by filtration, washed with hot water (20 mL). Finally, the crude product was recrystallized from ethanol to set pure product.

**Spectroscopic data of the synthesized compounds: (for spectra, see Supporting Information).** *2-Amino-4-(2-chloro-6-methoxyquinolin-3-yl)-7-methyl-5-oxo-4H,5H-pyrano[4,3-*b*]pyran-3 carbonitrile (Table 3 Entry 1, compd. code PA).* Red brown solid; yield 88%; mp >300°C; IR ( $\nu$  max): 3305.39, 3087.48, 2190.74, 1715.37, 1643.05, 1605.45  $\text{cm}^{-1}$ ; <sup>1</sup>H NMR (300 MHz, DMSO-*d*<sub>6</sub>): 2.223–2.396 (m, 3H, –CH<sub>3</sub>),  $\delta$ , 3.124 (s, 2H, –NH<sub>2</sub>), 3.869–3.981 (q, 3H, –OCH<sub>3</sub>), 4.784–4.883 (q, 1H, –CH), 5.954–6.025 (d, 1H, *J* = 21.3 Hz, Ar–H), 7.077–7.223 (q, 1H, *J* = 2.7 Hz, Ar–H), 7.280–7.385 (m, 1H, Ar–H), 7.870–7.914 (t, 1H, *J* = 9.3 Hz, Ar–H), 8.079–8.108 (d, 1H, *J* = 8.7 Hz, Ar–H) ppm; <sup>13</sup>C NMR (75 MHz, DMSO-*d*<sub>6</sub>):  $\delta$ , 19.76, 22.50, 31.69, 36.11, 55.90, 99.40, 115.80, 120.08, 120.71, 122.59, 123.25, 124.51, 127.82, 128.70, 130.12, 131.28, 141.20, 152.81, 163.20 ppm; mass (*m/z*): 395.79586 (M<sup>+</sup>). *Anal.* Calcd for C<sub>20</sub>H<sub>14</sub>ClN<sub>3</sub>O<sub>4</sub>: C, 60.69; H, 3.57; N, 10.62% Found: C, 60.62; H, 3.48; N, 10.55%.

*2-Amino-4-(4-formylphenyl)-7-methyl-5-oxo-4H,5H-pyrano[4,3-*b*]pyran-3-carbonitrile (Table 3 Entry 2, compd. code PB).* White solid; yield 84%; mp 270°C; IR ( $\nu$  max): 3194.51, 2925.48, 2197.49, 1698.02, 1673.91, 1642.09, 1612.20  $\text{cm}^{-1}$ ; <sup>1</sup>H NMR (300 MHz, DMSO-*d*<sub>6</sub>):  $\delta$ , 2.182 (s, 3H, –CH<sub>3</sub>), 4.245 (s, 1H, –CH), 6.015 (s, 1H, Ar–H), 6.645–6.746 (m, 6H, –NH<sub>2</sub>, Ar–H), 7.120–7.174 (q, 1H, *J* = 7.5 Hz, Ar–H), 7.805 (s, 1H, Ar–CHO) ppm; <sup>13</sup>C NMR (75 MHz, DMSO-*d*<sub>6</sub>):  $\delta$ , 19.91, 36.60, 55.17, 59.03, 98.34, 101.42, 112.18, 113.93, 119.45, 119.96, 129.56, 144.93, 158.42, 158.48, 159.61, 161.87, 162.48 ppm; mass (*m/z*): 308.28818 (M<sup>+</sup>). *Anal.* Calcd for C<sub>17</sub>H<sub>12</sub>N<sub>2</sub>O<sub>4</sub>: C, 66.23; H, 3.92; N, 9.09% Found: C, 66.04; H, 3.88; N, 8.96%.

*2-Amino-4-(7-fluoro-1-oxo-1,4-dihydronaphthalen-2-yl)-7-methyl-5-oxo-4H,5H-pyrano[4,3-*b*]pyran-3-carbonitrile (Table 3 Entry 3, compd. code PC).* Brown solid; yield 90%; mp >300°C; IR ( $\nu$  max): 3425.92, 3074.94, 2189.77, 1707.66, 1644.02, 1606.41  $\text{cm}^{-1}$ ; <sup>1</sup>H NMR (300 MHz, DMSO-*d*<sub>6</sub>):  $\delta$ , 2.150 (s, 3H, –CH<sub>3</sub>), 4.092 (s, 2H, –NH<sub>2</sub>), 6.031 (s, 1H, –CH), 6.579 (s, 2H, Ar–H), 7.395–7.421 (t, 1H, *J* = 4.8 Hz, Ar–H), 7.472–7.517 (t, 1H, *J* = 4.5 Hz, Ar–H), 7.567–7.605 (q, 1H, *J* = 3.0 Hz, Ar–H), 7.693 (s, 1H, Ar–H), 8.102 (s, 1H, Ar–H) ppm; <sup>13</sup>C NMR (75 MHz, DMSO-*d*<sub>6</sub>):  $\delta$ , 24.68, 35.67, 102.90, 103.37, 159.36, 164.90, 167.03, 167.37 ppm; mass (*m/z*): 364.3266232 (M<sup>+</sup>). *Anal.* Calcd for C<sub>20</sub>H<sub>13</sub>FN<sub>2</sub>O<sub>4</sub>: C,

65.93; H, 3.60; N, 7.69% Found: C, 65.86; H, 3.52; N, 7.54%.

**2-Amino-4-(5-bromo-2-hydroxyphenyl)-7-methyl-5-oxo-4H,5H-pyrano[4,3-b]pyran-3-carbonitrile (Table 3 Entry 4, compd. code PD).** White solid; yield 87%; mp 282°C; IR (v max): 3346.85, 3061.44, 2363.34, 1785.76, 1731.76, 1691.27  $\text{cm}^{-1}$ ;  $^1\text{H}$  NMR (300 MHz, DMSO-*d*<sub>6</sub>):  $\delta$ , 2.162 (s, 3H, CH<sub>3</sub>), 4.270 (s, 1H, —CH), 6.013 (s, 1H, —OH), 6.500 (s, 2H, NH<sub>2</sub>), 7.109–7.240 (m, 4H, Ar—H), 7.670 (s, 1H, Ar—H) ppm;  $^{13}\text{C}$  NMR (75 MHz, DMSO-*d*<sub>6</sub>):  $\delta$ , 19.17, 36.57, 58.50, 98.58, 101.13, 119.80, 127.52, 127.76, 128.82, 143.65, 158.64, 158.88, 162.19, 163.23 ppm; mass (*m/z*): 375.17354 (M<sup>+</sup>). *Anal.* Calcd for C<sub>16</sub>H<sub>11</sub>BrN<sub>2</sub>O<sub>4</sub>: C, 51.22; H, 2.96; N, 7.47% Found: C, 51.04; H, 2.84; N, 7.38%.

**2-Amino-4-(3-methoxyphenyl)-7-methyl-5-oxo-4H,5H-pyrano[4,3-b]pyran-3-carbonitrile (Table 3 Entry 5, compd. code PE).** White solid; yield 94%; mp 238°C; IR (v max): 3322.75, 3182.93, 3097.12, 2205.20, 1702.84, 1671.98, 1643.05, 1608.34  $\text{cm}^{-1}$ ;  $^1\text{H}$  NMR (300 MHz, DMSO-*d*<sub>6</sub>):  $\delta$ , 2.214 (s, 3H, —CH<sub>3</sub>), 3.728 (s, 3H, —OCH<sub>3</sub>), 4.237 (s, 1H, —CH), 6.208 (s, 1H, Ar—H), 6.713–6.789 (t, 3H, *J* = 9.3 Hz, Ar—H), 7.101 (s, 2H, Ar—H), 7.180–7.232 (t, 1H, *J* = 7.8 Hz, Ar—H) ppm;  $^{13}\text{C}$  NMR (75 MHz, DMSO-*d*<sub>6</sub>):  $\delta$ , 19.80, 36.58, 55.32, 58.35, 98.51, 101.10, 112.19, 114.09, 119.69, 119.92, 129.92, 145.34, 158.63, 158.74, 159.60, 162.02, 163.11 ppm; mass (*m/z*): 310.30406 (M<sup>+</sup>). *Anal.* Calcd for C<sub>17</sub>H<sub>14</sub>N<sub>2</sub>O<sub>4</sub>: C, 65.80; H, 4.55; N, 9.03% Found: C, 65.68; H, 4.46; N, 8.98%.

**2-Amino-4-(2-chlorophenyl)-7-methyl-5-oxo-4H,5H-pyrano[4,3-b]pyran-3-carbonitrile (Table 3 Entry 6, compd. code PF).** White solid; yield 90%; mp 268°C; IR (v max): 3338.18, 3103.87, 2190.74, 1748.16, 1698.02, 1671.02, 1632.45, 1605.45  $\text{cm}^{-1}$ ;  $^1\text{H}$  NMR (300 MHz, DMSO-*d*<sub>6</sub>):  $\delta$ , 2.228 (s, 3H, —CH<sub>3</sub>), 4.792 (s, 1H, —CH), 6.230 (s, 1H, Ar—H), 7.147 (s, 2H, Ar—H), 7.181–7.271 (m, 3H, —NH<sub>2</sub>, Ar—H), 7.342–7.366 (d, 1H, *J* = 7.2 Hz, Ar—H) ppm;  $^{13}\text{C}$  NMR (75 MHz, DMSO-*d*<sub>6</sub>):  $\delta$ , 19.82, 34.20, 57.00, 98.39, 100.02, 119.32, 127.88, 129.09, 129.98, 130.80, 132.88, 140.52, 158.77, 159.33, 161.77, 163.46 ppm; mass (*m/z*): 314.72314 (M<sup>+</sup>). *Anal.* Calcd for C<sub>16</sub>H<sub>11</sub>ClN<sub>2</sub>O<sub>3</sub>: C, 61.06; H, 3.52; N, 8.90% Found: C, 60.90; H, 3.48; N, 8.82%.

**2-Amino-4-(3-chlorophenyl)-7-methyl-5-oxo-4H,5H-pyrano[4,3-b]pyran-3-carbonitrile (Table 3 Entry 7, compd. code PG).** White solid; yield 93%; mp 256°C; IR (v max): 3392.17, 3322.75, 3195.47, 3096.15, 2196.52, 1704.76, 1671.98, 1644.02, 1613.16  $\text{cm}^{-1}$ ;  $^1\text{H}$  NMR (300 MHz, DMSO-*d*<sub>6</sub>):  $\delta$ , 2.219 (s, 3H), 4.311 (s, 1H), 6.226 (s, 1H), 7.139–7.198 (t, 3H, *J* = 7.5 Hz, —NH<sub>2</sub>, Ar—H), 7.231–7.258 (d, 1H, *J* = 8.1 Hz, Ar—H), 7.297–7.348 (t, 1H, *J* = 7.2 Hz, Ar—H) ppm; mass (*m/z*): 314.72314 (M<sup>+</sup>). *Anal.* Calcd for C<sub>16</sub>H<sub>11</sub>ClN<sub>2</sub>O<sub>3</sub>: C, 61.06; H, 3.52; N, 8.90% Found: C, 61.94; H, 3.56; N, 8.86%.

**2-Amino-4-(4-chlorophenyl)-7-methyl-5-oxo-4H,5H-pyrano[4,3-b]pyran-3-carbonitrile (Table 3 Entry 8, compd. code PH).** White solid; yield 92%; mp 232°C; IR (v max): 3380.60, 3322.75, 3194.51, 2200.38, 1712.48, 1644.02, 1611.23  $\text{cm}^{-1}$ ;  $^1\text{H}$  NMR (300 MHz, DMSO-*d*<sub>6</sub>):  $\delta$ , 1.586 (s, 3H, —CH<sub>3</sub>), 2.268 (s, 2H, —NH<sub>2</sub>), 4.479 (s, 1H, —CH), 5.928–5.930 (d, 1H, *J* = 0.6 Hz, Ar—H), 7.231–7.329 (m, 5H, Ar—H) ppm; mass (*m/z*): 314.72314 (M<sup>+</sup>). *Anal.* Calcd for C<sub>16</sub>H<sub>11</sub>ClN<sub>2</sub>O<sub>3</sub>: C, 61.06; H, 3.52; N, 8.90% Found: C, 60.98; H, 3.30; N, 8.84%.

**2-Amino-7-methyl-5-oxo-4-phenyl-4H,5H-pyrano[4,3-b]pyran-3-carbonitrile (Table 3 Entry 9, compd. code PI).** White solid; yield 88%; mp 236°C; IR (v max): 3392.17, 3320.82, 3181.00, 2197.49, 1704.76, 1671.98, 1642.09, 1612.20  $\text{cm}^{-1}$ ;  $^1\text{H}$  NMR (300 MHz, DMSO-*d*<sub>6</sub>):  $\delta$ , 2.212 (s, 3H, OCH<sub>3</sub>), 4.266 (s, 1H, —CH), 6.234 (s, 1H, Ar—H), 7.138–7.198 (t, 1H, *J* = 9.0 Hz, Ar—H), 7.231 (s, 3H, Ar—H), 7.274–7.321 (t, 2H, *J* = 7.2 Hz, —NH<sub>2</sub>) ppm; mass (*m/z*): 280.27808 (M<sup>+</sup>). *Anal.* Calcd for C<sub>16</sub>H<sub>12</sub>N<sub>2</sub>O<sub>3</sub>: C, 68.56; H, 4.32; N, 9.99% Found: C, 68.42; H, 4.10; N, 9.78%.

**2-Amino-4-(4-methoxyphenyl)-7-methyl-5-oxo-4H,5H-pyrano[4,3-b]pyran-3-carbonitrile (Table 3 Entry 10, compd. code PJ).** Yellow solid; yield 80%; mp 214°C; IR (v max): 3348.78, 3188.72, 3087.48, 2191.7, 1698.02, 1671.98, 1640.16, 1605.45  $\text{cm}^{-1}$ ;  $^1\text{H}$  NMR (300 MHz, DMSO-*d*<sub>6</sub>):  $\delta$ , 2.250 (s, 3H, —CH<sub>3</sub>), 3.794 (s, 3H, —OCH<sub>3</sub>), 4.445 (s, 1H, —CH), 5.910 (s, 2H, —NH<sub>2</sub>), 6.839–6.878 (m, 2H, Ar—H), 7.017–7.280 (m, 3H, Ar—H) ppm; mass (*m/z*): 310.30406 (M<sup>+</sup>). *Anal.* Calcd for C<sub>17</sub>H<sub>14</sub>N<sub>2</sub>O<sub>4</sub>: C, 65.80; H, 4.55; N, 9.03% Found: C, 65.77; H, 4.48; N, 8.94%.

**2-Amino-4-(4-cyanophenyl)-7-methyl-5-oxo-4H,5H-pyrano[4,3-b]pyran-3-carbonitrile (Table 3 Entry 11, compd. code PK).** White solid; yield 86%; mp 228°C; IR (v max): 3350.71 3192.58, 2929.34, 2228.3, 2274.63, 2200.38, 1724.05, 1678.73, 1647.88, 1610.27  $\text{cm}^{-1}$ ;  $^1\text{H}$  NMR (300 MHz, DMSO-*d*<sub>6</sub>):  $\delta$ , 1.600 (s, 3H, —CH<sub>3</sub>), 2.281 (s, 2H, —NH<sub>2</sub>), 4.784 (s, 1H, —CH), 7.418–7.445 (d, 1H, *J* = 8.1 Hz, Ar—H), 7.633–7.660 (d, 1H, *J* = 8.1 Hz, Ar—H), 7.838–7.868 (d, 2H, *J* = 9.0 Hz, Ar—H), 8.002–8.030 (d, 1H, *J* = 8.4 Hz, Ar—H) ppm; mass (*m/z*): 305.28754 (M<sup>+</sup>). *Anal.* Calcd for C<sub>17</sub>H<sub>11</sub>N<sub>3</sub>O<sub>3</sub>: C, 66.88; H, 4.28; N, 8.94% Found: C, 66.76; H, 4.14; N, 8.82%.

**2-Amino-4-(3-bromophenyl)-7-methyl-5-oxo-4H,5H-pyrano[4,3-b]pyran-3-carbonitrile (Table 3 Entry 12, compd. code PL).** White solid; yield 83%; mp 216°C; IR (v max): 3320.82, 3193.54, 3103.87, 2197.49, 1703.8, 1671.98, 1643.05, 1613.16  $\text{cm}^{-1}$ ;  $^1\text{H}$  NMR (300 MHz, DMSO-*d*<sub>6</sub>):  $\delta$ , 2.218 (s, 3H, —CH<sub>3</sub>), 2.530 (s, 2H, —NH<sub>2</sub>), 4.303 (s, 1H, —CH), 6.235 (s, 1H, Ar—H), 7.207 (s, 1H, Ar—H), 7.265–7.340 (t, 1H, *J* = 7.5 Hz, Ar—H), 7.381–7.406 (d, 1H, *J* = 7.5 Hz, Ar—H) ppm; mass (*m/z*):

359.17414 ( $M^+$ ). *Anal.* Calcd for  $C_{16}H_{11}BrN_2O_3$ : C, 53.50; H, 3.09; N, 7.80% Found: C, 53.38; H, 2.98; N, 7.74%.

**2-Amino-4-(2H-1,3-benzodioxol-5-yl)-7-methyl-5-oxo-4H,5H-pyrano[4,3-*b*]pyran-3-carbonitrile (Table 3 Entry 13, compd. code PM).** White solid; yield 92%; mp 264°C; IR (v max): 3320.82, 3193.54, 3103.87, 2197.49, 1703.8, 1671.98, 1643.05, 1613.16  $cm^{-1}$ ;  $^1H$  NMR (300 MHz, DMSO-*d*<sub>6</sub>):  $\delta$ , 1.646 (s, 3H,  $-CH_3$ ), 4.408 (s, 1H,  $-CH$ ), 4.688 (s, 1H, Ar-H), 5.914–5.943 (d, 2H,  $-NH_2$ ), 6.099–6.145 (d, 2H,  $J = 8.7$  Hz,  $-CH_2$ ), 6.741–6.820 (m, 1H, Ar-H), 6.934–6.961 (d, 1H,  $J = 8.1$  Hz, Ar-H), 7.280–7.617 (m, 1H, Ar-H), 7.624 (s, 1H, Ar-H), ppm; mass ( $m/z$ ): 324.28758 ( $M^+$ ). *Anal.* Calcd for  $C_{17}H_{12}N_2O_5$ : C, 62.96; H, 2.78; N, 8.64% Found: C, 62.90; H, 2.82; N, 8.58%.

**Acknowledgments.** One of the authors Miss Priyanka Mohire thanks the Department of Science and Technology New Delhi, Govt. of India for the award of INSPIRE fellowship (JRF-IF150988) for financial support. We gratefully acknowledge Department of Chemistry, Shivaji University, Kolhapur, for providing NMR spectral analysis.

#### REFERENCES AND NOTES

- [1] Raviglionea, M. C. *Bull World Health Organ* 2007, 85(5), 327.
- [2] Mallowney, M. W.; Hwang, C. H.; Newsome, A. G.; Wei, X.; Tanouye, U.; Wan, B.; Carlson, S.; Barranis, N. J.; Ainmhire, E.; Chen, W. L.; Krishnamoorthy, K.; White, J.; Blair, R.; Lee, H.; Burdette, J. E.; Rathod, P. K.; Parish, T.; Cho, S.; Franzblau, S. G.; Murphy, B. T. *ACS Infect Dis* 2015, 1, 168.
- [3] Moraski, G. C.; Seeger, N.; Miller, P. A.; Oliver, A. G.; Boshoff, H. I.; Cho, S.; Mulugeta, S.; Anderson, J. R.; Franzblau, S. G.; Miller, M. J. *ACS Infect Dis* 2016, 2, 393. <https://doi.org/10.1021/acinfecdis.5b00154>.
- [4] World Health Organization (WHO), *Global Tuberculosis Report 2016*; WHO: 2016.
- [5] Chen, C.; Lu, M.; Liu, Z.; Wan, J.; Tu, Z.; Zhang, T.; Yan, M. *Open J Med Chem* 2013, 3, 128.
- [6] Saleshier, F. M.; Suresh, S.; Anitha, N.; Karim, J.; Divakar, M. *C. Eur J Exp Biol* 2011, 1, 150.
- [7] Manvar, A.; Malde, A.; Verma, J.; Virsodia, V.; Mishra, A.; Upadhyay, K.; Acharya, H.; Coutinho, E.; Shah, A. *Eur J Med Chem* 2008, 43, 2395.
- [8] Massengo-Tiass, R. P.; Cronan, J. E. *Cell Mol Life Sci* 2009, 66, 1507.
- [9] Rozwarski, D. A.; Vilcheze, C.; Sugantino, M.; Bittman, R.; Sacchettini, J. C. *J Biol Chem* 1999, 274, 15582.
- [10] Marrakchi, H.; Laneelle, G.; Quemard, A. *Microbiology* 2000, 146, 289.
- [11] Jeyachandran, M.; Ramesh, P.; Sriram, D.; Senthilkumar, P.; Yogeewari, P. *Bioorg Med Chem Lett* 2012, 22, 4807.
- [12] Lilienkampf, A.; Mao, J.; Wan, B.; Wang, Y.; Franzblau, S. G.; Kozikowski, A. P. *J Med Chem* 2009, 52, 2109.
- [13] Copp, B. R.; Pearce, A. N. *Nat Prod Rep* 2003, 20, 535.
- [14] Gore, R. P.; Rajput, A. P. *Drug Invention Today* 2013, 5, 148.
- [15] (a) Biggs-Houck, J. E.; Younai, A.; Shaw, J. T. *Curr Opin Chem Biol* 2010, 14, 371; (b) Mohire, P. P.; Patil, R. B.; Chandam, D. R.; Jadhav, S. J.; Patravale, A. A.; Kumbhar, D. R.; Ghosh, J. S.; Deshmukh, M. B. *Res Chem Intermed* 2017, 43, 7013; (c) Patravale, A. A.; Gore, A. H.; Patil, D. R.; Kolekar, G. B.; Deshmukh, M. B.; Choudhari, P. B.; Bhatia, M. S.; Anbhule, P. V. *Res Chem Intermed* 2016, 42, 2919.
- [16] Gu, Y. *Green Chem* 2012, 14, 2091.
- [17] Valizadeh, H.; Fakhari, A. *Mol Divers* 2011, 15, 233.
- [18] Praveen Kumar, P.; Dathu Reddy, Y.; Venkata Ramana Reddy, C.; Rama Devi, B.; Dubey, P. K. *Tetrahedron Lett* 2014, 55, 2177.
- [19] Patel, D. S.; Avalani, J. R.; Raval, D. K. *J Saudi Chem Soc* 2016, 20, S401.
- [20] Khoobia, M.; Ma'mania, L.; Rezazadehb, F.; Zareieb, Z.; Foroumadi, A.; Ramazanib, A.; Shafieec, A. *J Mol Cat A: Chemical* 2012, 359, 74.
- [21] Greaves, T. L.; Drummond, C. *J Chem Rev* 2015, 115, 11379.
- [22] Otaibi, A. A.; Cluskey, A. M. *Multicomponent Reactions in Ionic Liquids; Ionic Liquids - New Aspects for the Future*; Kadokawa, J. Ed.; InTech, 2013. <https://doi.org/10.5772/51937>. Available from: <https://www.intechopen.com/books/ionic-liquids-new-aspects-for-the-future/multicomponent-reactions-in-ionic-liquids>
- [23] Watanabe, H.; Doi, H.; Saito, S.; Matsugami, M.; Fujii, K.; Kanzaki, R.; Kameda, Y.; Umebayashi, Y. *J Mol Liq* 2016, 217, 35.
- [24] Henderson, L. C.; Thornton, M. T.; Byrne, N.; Fox, B. L.; Waugh, K. D.; Squire, J. S.; Servinis, L.; Delaney, J. P.; Brozinski, H. L.; Andrighetto, L. M.; Altimari, J. M. *C R Chimie* 2013, 16, 634.
- [25] Baghbanian, S. M.; Farhang, M. *J Mol Liq* 2013, 183, 45.
- [26] Song, Y.; Ke, H.; Wang, N.; Wang, L.; Zou, G. *Tetrahedron* 2009, 65, 9086.
- [27] Chen, X.; Liu, R.; Xu, Y.; Zou, G. *Tetrahedron* 2012, 68, 4813.
- [28] Gordon, C. P.; Byrne, N.; McCluskey, A. *Green Chem* 2010, 12, 1000.
- [29] Cota, I.; Medina, F.; Olmos, R. G.; Iglesias, M. *C R Chimie* 2014, 17, 18.
- [30] Henderson, L. C.; Byrne, N. *Green Chem* 2011, 13, 813.
- [31] Baghbanian, S. M.; Tajbakhsh, M.; Farhang, M. *C R Chimie* 2014, 17, 1160.
- [32] Tajbakhsh, M.; Alinezhad, H.; Norouzi, M.; Bagheri, S.; Akbari, M. *J Mol Liq* 2013, 177, 44.
- [33] Mulik, A. G.; Chandam, D. R.; Patil, D. R.; Patil, P. P.; Mulik, G. N.; Salunkhe, S. T.; Deshmukh, M. B. *Res Chem Intermed* 2015, 41, 10085.
- [34] Isambert, N.; Duque, M. D. M. S.; Plaquevent, J. C.; Genisson, Y.; Rodriguez, J.; Constantieux, T. *Chem Soc Rev* 2011, 40, 1347.
- [35] Marsh, N.; Boxall, J. A.; Lichtenthaler, R. *Fluid Phase Equilib* 2004, 219, 93.
- [36] Welton, T. *Chem Rev* 1999, 99, 2071.
- [37] Uher, M.; Konecny, V.; Rajniakova, O. *Chem Papers* 1994, 48(4), 282.
- [38] Ronad, P. M.; Noolvi, M. N.; Sapkal, S.; Dharbhamulla, S.; Maddi, V. S. *Eur J Med Chem* 2010, 45, 85.
- [39] Fan, X.; Feng, D.; Qua, Y.; Zhang, X.; Wang, J.; Loiseau, P. M.; Andrei, G.; Snoeck, R.; Clercq, E. D. *Bioorg Med Chem Lett* 2010, 20, 809.
- [40] Aytemir, M. D.; Calis, U.; Ozalp, M. *Arch Pharm Pharm Med Chem* 2004, 337, 281.
- [41] El-Saghier, M. M.; Naili, M. B.; Rammash, B. K.; Saleh, N. A.; Kreddanc, K. M. *ARKIVOC* 2007, 16, 83.
- [42] Kalaria, P. N.; Satasia, S. P.; Raval, D. K. *New J Chem* 2014, 38, 1512.
- [43] Manvar, A.; Bavishi, A.; Radadiya, A.; Patel, J.; Vora, V.; Dodia, N.; Rawal, K.; Shah, A. *Bioorg Med Chem Lett* 2011, 21, 4728.
- [44] Mungra, D. C.; Patel, M. P.; Rajani, D. P.; Patel, R. G. *Eur J Med Chem* 2011, 46, 4192.
- [45] Kamdar, N. R.; Haveliwala, D. D.; Mistry, P. T.; Patel, S. K. *Eur J Med Chem* 2010, 45, 5056.
- [46] (a) Rahmati, A.; Khalesi, Z.; Kenarkoobi, T. *Comb Chem High Throughput Screen* 2014, 17, 132; (b) Habibi, M.; Habibi, A.; Nasab, S. H.; Dolati, H.; Mahdavi, S. M. *J Heterocycl Chem* 2016, 54, 1598; (c) Chalapala, S.; Bandi, R.; Chinnachennaiahgari, V. B.; Perali, R. S. *Tetrahedron* 2017, 73, 3923.

- [47] Stoyanova, E. V.; Ivanova, I. C.; Heberb, D. *Molecules* 2000, 5, 19.
- [48] Wang, X.; Zhou, J. X.; Zeng, Z. S.; Li, Y. L.; Shi, D. Q.; Tua, S. J. *ARKIVOC* 2006, 11, 107.
- [49] Shaabani, A.; Samadi, S.; Badri, Z.; Rahmati, A. *Catal Lett* 2005, 104, 39.
- [50] Seifi, M.; Sheibani, H. *Catal Lett* 2008, 126, 275.
- [51] Rajguru, D.; Keshwal, B. S.; Jain, S. *Chin Chem Lett* 2013, 24, 1033.
- [52] Khaligh, N. G. *Monatsh Chem* 1643, 2014, 145.
- [53] Ghashang, M.; Mansoor, S. S.; Aswin, K. *Chin J Catal* 2014, 35, 127.
- [54] Khaligh, N. G.; Abd Hamid, S. B. *Chin J Catal* 2015, 36, 728.
- [55] Kinen, C. O.; Rossi, L. I.; Rossi, R. H. *Green Chem* 2009, 11, 223.
- [56] Andraos, J. *Org Process Res Dev* 2005, 9, 404.
- [57] (a) Chandam, D. R.; Patravale, A. A.; Jadhav, S. J.; Deshmukh, M. B. *J Mol Liq* 2017, 240, 98; (b) Vibhute, S.; Jamale, D.; Undare, S.; Valekar, N.; Kolekar, G.; Anbhule, P. *Res Chem Intermed*, 43, 4561. <https://doi.org/10.1007/s11164-017-2896-5>; (c) Jadhav, S.; Patravale, A.; Patil, R.; Kumbhar, D.; Karande, V.; Chandam, D.; Deshmukh, M. *Current Green Chem* 2016, 3, 227.
- [58] Mukhopadhyay, C.; Datta, A. *J Heterocyclic Chem* 2009, 46, 91.
- [59] Curzons, A. D.; Constable, D. J. C.; Mortimera, D. N.; Cunninghamb, V. L. *Green Chem* 2001, 3, 1.
- [60] Lourenco, M. C. S.; Nora de Souza, M. V.; Pinheiro, A. C.; de L. Ferreira, M.; Goncalves, R. B.; Nogueira, T. C. M.; Peralta, M. A. *ARKIVOC* 2007, 15, 181.
- [61] Tortoli, E.; Cichero, P.; Piersimoni, C.; Simonetti, M. T.; Gesu, G.; Nista, D. *J Clin Microbiol* 1999, 37, 3578.
- [62] Trott, O.; Olson, A. J. *J Comput Chem* 2010, 31, 455.
- [63] Accelrys Software Inc, *Discovery Studio Modelling Environment, Releaser 4.0 San Diego: Accelrys Software inc.* 2013.

## SUPPORTING INFORMATION

Additional Supporting Information may be found online in the supporting information tab for this article.